Observing pure effects of counter-rotating terms without ultrastrong coupling: A single photon can simultaneously excite two qubits

Xin Wang,[1,2] Adam Miranowicz,[2,3,*] Hong-Rong Li,[1,†] and Franco Nori[2,4]

[1]*Institute of Quantum Optics and Quantum Information, School of Science, Xi'an Jiaotong University, Xi'an 710049, China*

[2]*CEMS, RIKEN, Wako-shi, Saitama 351-0198, Japan*

[3]*Faculty of Physics, Adam Mickiewicz University, 61-614 Poznań, Poland*

[4]*Physics Department, The University of Michigan, Ann Arbor, Michigan 48109-1040, USA*

(Received 15 September 2017; published 14 December 2017)

The coherent process that a single photon simultaneously excites two qubits has recently been theoretically predicted by Garziano *et al.* [L. Garziano, V. Macrì, R. Stassi, O. Di Stefano, F. Nori, and S. Savasta, One Photon Can Simultaneously Excite two or More Atoms, Phys. Rev. Lett. **117**, 043601 (2016)]. We propose a different approach to observe a similar dynamical process based on a superconducting quantum circuit, where two coupled flux qubits longitudinally interact with the same resonator. We show that this simultaneous excitation of two qubits (assuming that the sum of their transition frequencies is close to the cavity frequency) is related to the counter-rotating terms in the dipole-dipole coupling between two qubits, and the standard rotating-wave approximation is not valid here. By numerically simulating the adiabatic Landau-Zener transition and Rabi-oscillation effects, we clearly verify that the energy of a single photon can excite two qubits via higher-order transitions induced by the longitudinal couplings and the counter-rotating terms. Compared with previous studies, the coherent dynamics in our system only involves one intermediate state and, thus, exhibits a much faster rate. We also find transition paths which can interfere. Finally, by discussing how to control the two longitudinal-coupling strengths, we find a method to observe both constructive and destructive interference phenomena in our system.

DOI: 10.1103/PhysRevA.96.063820

I. INTRODUCTION

The light-matter interaction between a quantized electromagnetic field and two-level atoms has been the central topic of quantum optics for half a century, and has developed into the standard cavity quantum electrodynamics (QED) theory. In a QED system, if the dipole-field or dipole-dipole coupling strengths (λ) are weak compared with the cavity or atomic transition frequencies (ω_c and ω_q, respectively), we often routinely adopt the rotating-wave approximation (RWA). Under the RWA, one can neglect the excitation-number-nonconserving terms [1–4], which, compared with the resonant terms, are usually only rapidly oscillating virtual processes and negligibly contribute to the dynamical evolution of such a system [5].

In fact, the RWA works well even in the strong-coupling regime. Only in the ultrastrong- and deep-strong-coupling regimes [where $\lambda > 0.1 \times \min(\omega_c,\omega_q)$ and $\lambda > \min(\omega_c,\omega_q)$, respectively] [6–14], the counter-rotating terms have apparent effects in a QED system [15,16]. The excitation-number-nonconserving terms in a QED system can lead to many interesting quantum effects [8,17–23], such as three-photon resonances [24], the modification of the standard input-output relation [25,26], quantum phase transitions [27], frequency conversion [28], or the deterioration of photon blockade effects [29,30]. However, all of these phenomena are the combined and mixed effects of both counter-rotating and resonant terms. Here we address, in particular, the following questions: How can we observe some pure effects of counter-rotating wave terms in a QED system, i.e., without being disturbed by the resonant terms? Moreover, is it really always reasonable to apply the RWA in dipole-field or dipole-dipole coupling systems, which are far away from the ultrastrong-coupling regime?

Other interesting quantum processes are multiexcitation and emission in a QED system. The process in which a two-level atom (molecule) absorbs two or more photons simultaneously has been widely discussed in many quantum platforms [14,22,23,31,32]. However, the inverse process (of a single photon splitting to excite two and more atoms) is rarely studied [33–35].

Recently, Garziano *et al.* [33] predicted that *one photon can simultaneously excite two or more qubits*. In their theoretical proposal, two superconducting qubits are coupled to a resonator with both longitudinal and transverse forms in the ultrastrong-coupling regime. A similar process was predicted via the photon-mediated Raman interactions between two three-level atoms (qutrits) in the strong-coupling regime [36]. Note that both dynamics (with qubits [33] and qutrits [36]) were composed of three virtual processes, which do not conserve the number of excitations. Also the effective transition between atoms and a single photon is of a relatively slow rate.

In this paper, we propose a superconducting system composed of a transmission-line resonator longitudinally coupled with two flux qubits. The two qubits couple to each other via an antiferromagnetic dipole-dipole interaction. We show that when the sum of two qubits' transition frequencies is approximately equal to the resonator frequency, the counter-rotating terms in the dipole-dipole interaction cannot be dropped even when the system has not entered into the ultrastrong-coupling regime. The RWA is not valid here; on the

*miran@amu.edu.pl

†hrli@mail.xjtu.edu.cn

contrary, the resonant terms can be approximately neglected in our model. Due to the counter-rotating terms, a single photon in the resonator can simultaneously excite two qubits. Finally, we discuss the quantum interference effects between four transition paths. Compared with the similar dynamics studied in Refs. [33,36], the whole transition process proposed now only involves a *single* intermediate step and the process rate can be much faster. Additionally, our proposal does not require one to induce *both* longitudinal and transverse couplings [33], so the superconducting qubit can work at the optimal point and, thus, the pure-dephasing rate of the qubits can be effectively suppressed [22,23,37,38]. Moreover, we consider *qubits instead of the qutrits* studied in Ref. [36]. By discussing the parameters in our system, we find that the coherence rate can easily exceed the decoherence rate, and it is possible to observe these quantum effects with current experimental setups.

Superconducting circuits with Josephson qubits are a suitable platform to explore our proposal, as will be discussed in detail in Sec. II. We note that the past few years have witnessed the rapid development in quantum control and quantum engineering based on superconducting quantum circuits [16,39–47]. The current manufacturing, control, and detection technologies for the superconducting devices are mature [48–52]. Many quantum phenomena in atomic physics and quantum optics, such as vacuum Rabi oscillations [16], Autler-Townes splitting [53–55], and Fock states generation [56–58], have been demonstrated based on superconducting quantum circuits [16]. Moreover, since the dipole moments of a superconducting qubit are extremely large compared with the ones in natural atoms, the coupling strength in a circuit QED system [46,59] can enter into the strong, ultrastrong [7,8,11,12,14], and even deep-strong [13] regimes. All these advantages make superconducting quantum circuits an ideal platform for exploring various quantum effects beyond the RWA.

II. MODEL

Our model can be implemented in a superconducting quantum circuit layout with Josephson junctions. As shown in Fig. 1, we consider two gap-tunable flux qubits [37,38,60–63] placed in a transmission-line resonator (TLR), and coupled together with an antiferromagnetic interaction [64–66]. The Hamiltonian for the two qubits is expressed as (setting $\hbar = 1$)

$$\bar{H}_q = \frac{1}{2}\sum_{j=1}^{2}\left(\Delta_j\bar{\sigma}_j^x + \epsilon_j\bar{\sigma}_j^z\right) + J\bar{\sigma}_1^z\bar{\sigma}_2^z, \tag{1}$$

where the energy basis $\epsilon_j = 2I_{p,j}(\Phi_j^z - \Phi_0/2)$ can be controlled via the flux Φ_j^z through the two symmetric gradiometric loops [38,63], Δ_j is the energy gap, Φ_0 is the flux quantum, and $\bar{\sigma}_z^j$ and $\bar{\sigma}_x^j$ are the Pauli operators for the jth qubit in the basis of persistent current states: $|\uparrow_j\rangle$ (counterclockwise) and $|\downarrow_j\rangle$ (clockwise) with amplitude $I_{p,j}$ [60,61]. The dipole-dipole interaction strength J is given by $J = M_q I_{p,1} I_{p,2}$, where M_q is the mutual inductance between two qubits [64–66]. For such a layout arrangement, the mutual inductance M_q and coupling strength J are determined by the geometry and spatial relation, when the qubits are placed next to each other. Alternatively, as discussed in Refs. [67–70], one can achieve a tunable indirect coupling by employing a coupler, which allows a flexible coupling between two distant qubits. Here we just assume the two flux qubits as an example, and they can be replaced by some other type of superconducting artificial qubits (see, e.g., Figs. 1 and 2 in Ref. [16]).

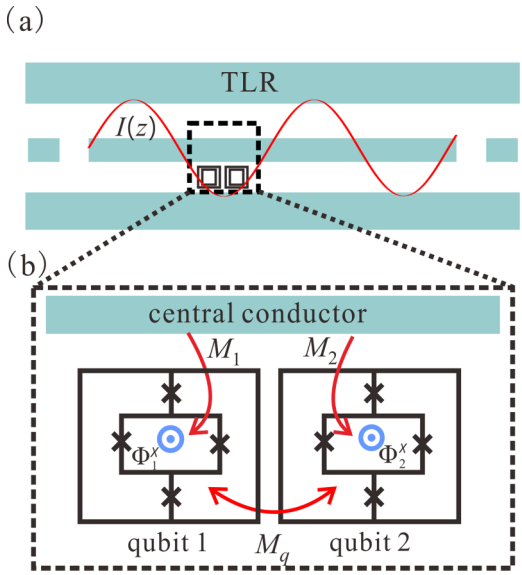

FIG. 1. (a) Schematic circuit layout of our proposal. The central conductor of the transmission-line resonator (TLR) is stretched in the z direction, and the two flux qubits are placed at the antinode positions of the TLR standing-wave current $I(z)$. Here we assume that each qubit is composed of two symmetric gradiometric loops and a SQUID loop. (b) The quantized current $I(z)$ through the TLR central conductor can interact with the first and second qubit SQUID loops via mutual inductances M_1 and M_2, respectively. Each qubit is composed of four Josephson junctions (modeled by black crosses). To bias the energy gap of each qubit, a static flux Φ_j^x must be through the jth SQUID loop. The two qubits couple together with their mutual inductance M_q.

The energy gap Δ_j can be controlled conveniently by adjusting the static flux Φ_j^x through the superconducting quantum interference device (SQUID) loop. Since the sizes of two qubits ($\sim 10\ \mu$m) are negligible compared with the TLR wavelength ($\sim$cm), we assume that the resonator current is independent of the resonator position and the dipole approximation is valid here. The qubits are placed at the antinode position z_0 of the TLR current [16,46,59]. Since each qubit has two symmetric gradiometric loops, the flux contribution from the current $I(z)$ in the central conductor of the TLR vanishes to the first order of the energy bias ϵ_j [37,38,63]. However, the current $I(z)$ in the central conductor of the TLR can produce flux perturbations to the SQUID loop of the jth qubit via the mutual inductance M_j [37,63]. Therefore, Δ_j can be expressed as

$$\Delta_j = \Delta_j\left(\Phi_{j0}^x\right) + R_j M_j I(z_0), \tag{2}$$

where $R_j = \partial\Delta_j(\Phi_j^x)/\partial\Phi_j^x$ is the sensitivity of the energy gap Δ_j on the static-flux frustration at the position Φ_{j0}^x [37,63]. The quantized current of the TLR can be directly obtained from

the quantization of the voltage and expressed as [16,59,71,72]

$$I(z_0) = \sqrt{\frac{\omega}{2L_0 L}}(a + a^\dagger), \tag{3}$$

where L_0 is the inductance per unit length of the TLR, a ($a^\dagger$) denotes the annihilation (creation) operator of a microwave photon in the TLR, ω is the resonant mode frequency considered here, and L is the total length of the resonator [59,71]. The coupling strength between the jth qubit and a single microwave photon in the resonator has the form

$$g_j = R_j M_j \sqrt{\frac{\omega}{2L_0 L}}, \tag{4}$$

and the total Hamiltonian for the whole system can be written as

$$\bar{H}_T = \omega a^\dagger a + \frac{1}{2}\sum_{j=1}^{2}\left(\Delta_j \bar{\sigma}_j^x + \epsilon_j \bar{\sigma}_j^z\right) + \sum_{j=1}^{2} g_j \bar{\sigma}_j^x (a + a^\dagger) + J\bar{\sigma}_1^z \bar{\sigma}_2^z. \tag{5}$$

In an experiment, if we apply static fluxes Φ_1^x and Φ_2^x through the SQUID loop of two qubits with the opposite (same) direction, the flux sensitivities of the energy gaps R_1 and R_2 are of the opposite (same) sign. Moreover, by setting the jth qubit working at different energy-gap points Δ_j, the amplitude of R_1 and R_2 can be easily modified [37,63]. It can be found that R_1 and R_2 directly determine the strengths and relative sign between g_1 and g_2. The coupling strengths between the qubits and resonator can be conveniently adjusted in this circuit QED system according to Eq. (4). In Sec. IV, we demonstrate how to obtain different interference effects by modifying R_1 and R_2.

To minimize the pure dephasing effect of two qubits induced by the flux noise, we often operate the qubits at their optimal points with $\epsilon_j = 2I_{p,j}(\Phi_j^z - \Phi_0/2) = 0$, by applying a static flux $\Phi_j^z = \Phi_0/2$ [38,63] through two gradiometric loops. In the new basis of the eigenstates $|e_j\rangle = (|\uparrow_j\rangle + |\downarrow_j\rangle)\sqrt{2}$ and $|g_j\rangle = (|\uparrow_j\rangle - |\downarrow_j\rangle)\sqrt{2}$, we can rewrite the Hamiltonian in Eq. (5) as

$$H_T = \omega a^\dagger a + \frac{1}{2}\sum_{j=1}^{2}\Delta_j \sigma_j^z + \sum_{j=1}^{2} g_j \sigma_j^z (a + a^\dagger) + J\sigma_1^x \sigma_2^x, \tag{6}$$

where $\sigma_j^z = |e_j\rangle\langle e_j| - |g_j\rangle\langle g_j|$ and $\sigma_j^x = \sigma_j^+ + \sigma_j^- = |e_j\rangle\langle g_j| + |g_j\rangle\langle e_j|$. It can be found that the qubit-resonator coupling is of a longitudinal form, rather than that in the Rabi model for standard QED systems.

In this paper, we assume that two qubits are nearly resonant, i.e., $\Delta_1 \backsimeq \Delta_2$, but all our discussions here can be applied to the case when the two qubits are far off resonance. The last term in Eq. (6) describes the dipole-dipole interaction between two artificial atoms, which can be separated into two parts, i.e., the excitation-number-conserving terms,

$$H_{\rm R} = J(\sigma_1^- \sigma_2^+ + \text{H.c.}), \tag{7}$$

and the counter-rotating terms,

$$H_{\rm CR} = J(\sigma_1^+ \sigma_2^+ + \text{H.c.}). \tag{8}$$

It is known that $H_{\rm CR}$ describes an excitation-number-nonconserving process that two excitations are created (annihilated) at the same time. This virtual process happens with an extremely low probability at a rapid oscillating rate [5]. In a conventional analysis of such dipole-dipole coupling dynamics, the evolution of the two resonant qubits is dominated by the excitation-number-conserving term $H_{\rm R}$ before the coupling strength J enters into the ultrastrong-coupling regime. The counter-rotating term $H_{\rm CR}$ is only significant when the coupling reaches the ultrastrong- or deep-strong-coupling regimes. However, in this work, we find the interesting phenomenon that $H_{\rm CR}$, rather than $H_{\rm R}$, dominates the evolution process even *without* considering the ultrastrong-coupling regime, i.e., $\max\{J, g_i\} < 0.1 \times \min\{\omega, \Delta_j\}$.

III. HOW TO OBSERVE PURE EFFECTS OF COUNTER-ROTATING TERMS

We are interested in the regime when $\omega \approx \Delta_1 + \Delta_2$, and assume that the resonator and second-qubit frequencies are $\omega = 2\Delta_2 = 8$ GHz. Under current experimental conditions, the coupling strength between a TLR and a qubit can easily reach the strong-coupling regime (see Ref. [16] for a recent review) and we assume that $g_1 = g_2 = 0.2$ GHz. According to Ref. [73], a direct inductive coupling strength between the two flux qubits can be several-hundred MHz. In the following discussions, we set $J = 0.1$ GHz.

A. Anticrossing point in energy spectra

In Fig. 2(a), by changing the first atomic-transition frequency Δ_1, we plot the energy spectrum of the third and fourth eigenenergies by numerically solving the eigenproblem $H_T|\psi_n\rangle = E_n|\psi_n\rangle$, with $n = 3,4$. It can be seen that the two energy levels exhibit anticrossing with a splitting around $\Delta_1 = 4$ GHz (red solid curves), which indicates that there might be two states coupled resonantly. Specifically, if the counter-rotating terms $H_{\rm CR}$ in Eq. (6) are neglected, the anticrossing point disappears (see the dashed black curves). However, without the two-qubit resonant coupling terms $H_{\rm R}$, the energy spectrum (blue dot curves) for the third and fourth eigenstates coincides with the full Hamiltonian case, which indicates that the resonant coupling is due to the counter-rotating terms $H_{\rm CR}$ and has no relation to $H_{\rm R}$. We note that the predicted level anticrossing is analogous to that observed in the experiment of Niemczyk *et al.* [8] and other experiments in the ultrastrong-coupling (USC) regime using superconducting quantum circuits (for a very recent review, see [16] and references therein). Analogous to our model, the emergence of this level anticrossing needs qubit-oscillator longitudinal couplings. However, as discussed in Refs. [8,22,23], the origin of this phenomenon is due to multiexcitation processes and has a close relation to both the counter-rotating terms and Jaynes-Cummings (JC) terms in the transverse coupling. In our proposal, only the counter-rotating terms contribute to the energy-level anticrossing, even far below the USC regime.

In Fig. 2(b), we plot the probabilities $P_1 = |\langle 0,e,e|\psi_4\rangle|^2$, $P_2 = |\langle 1,g,g|\psi_4\rangle|^2$, $P_{s+} = |\langle S_+|\psi_3\rangle|^2$ and $P_{s-} = |\langle S_-|\psi_4\rangle|^2$ (where $|S_\pm\rangle = (|0,e,e\rangle \pm |1,g,g\rangle)/\sqrt{2}$), changing with Δ_1. It can be seen that $|\psi_3\rangle \simeq |1,g,g\rangle$ ($|\psi_4\rangle \simeq |0,e,e\rangle$) when $\Delta_1 \sim$

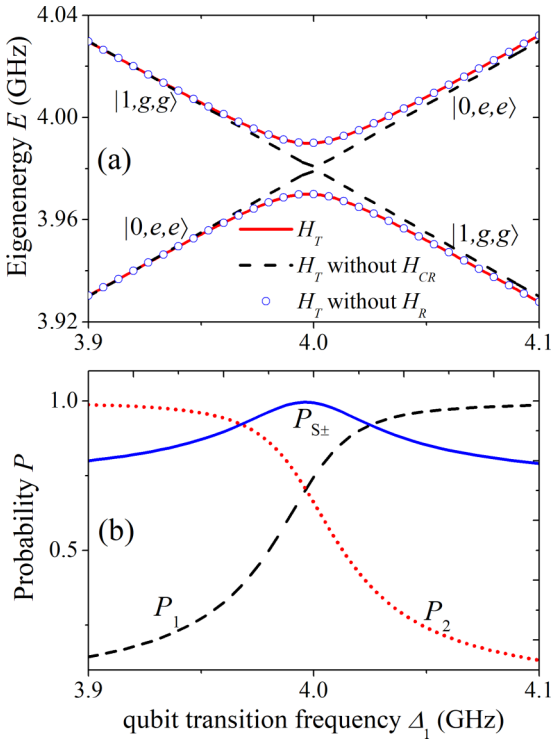

FIG. 2. (a) Eigenenergies E_3 and E_4 as functions of the first-qubit transition frequency Δ_1. Numerical results are calculated with the original Hamiltonian H_T in Eq. (6) (red solid curve), H_T without the counter-rotating terms $H_{\rm CR}$ (black dashed curve), and H_T without the resonant terms $H_{\rm R}$ (blue dots). It can be clearly seen that the energy spectrum for E_3 and E_4 exhibits an anticrossing point around $\Delta_1 = 4$ GHz. The results without $H_{\rm R}$, rather than without the counter-rotating terms $H_{\rm CR}$, match well with those of the original Hamiltonian H_T. (b) The probabilities P_1 (black dashed curve), P_2 (red dot curve), and $P_{s\pm}$ (blue solid curve) which are defined in Sec. III A, as functions of the first-qubit transition frequency Δ_1. The parameters used here are $\omega = 2\Delta_2 = 8$ GHz, $g_1 = g_2 = 0.2$ GHz, and $J = 0.1$ GHz.

3.9 GHz ($\Delta_1 \sim 4.1$ GHz). Around the anticrossing point, $|S_+\rangle \simeq |\psi_3\rangle$ and $|S_-\rangle \simeq |\psi_4\rangle$. One may wonder why we are not showing in Fig. 2 the corresponding plots for the probabilities $P_1' = |\langle 1,g,g|\psi_3\rangle|^2$, $P_2' = |\langle 0,e,e|\psi_3\rangle|^2$, $P_1' \approx P_1$, $P_2' \approx P_2$, such that we would not see any differences between the corresponding curves on the scale of Fig. 2. Therefore, we can conclude that the anticrossing point is due to the resonant coupling between the states $|0,e,e\rangle$ and $|1,g,g\rangle$. The coherent transfer between these two states corresponds to the same interesting process discussed in Ref. [33]: that a single photon in a cavity can excite two atoms simultaneously. One may wonder how this process can happen in our system with only longitudinal coupling. To show this, hereafter, we analytically derive its effective Hamiltonian.

B. Effective Hamiltonian for the tripartite interaction

We first perform the polariton transformation of the Hamiltonian $H_{\rm tot}$ in Eq. (6) given by

$$H_{s1} = e^{S} H_T e^{-S}, \tag{9}$$

with $S = \sum_{j=1}^{2} \beta_j \sigma_j^z (a^\dagger - a)$, where $\beta_j = g_j/\omega$ is the Lamb-Dicke parameter for the jth qubit-resonator longitudinal coupling. Thus, we obtain

$$H_{s1} = \omega a^\dagger a + \frac{1}{2}\sum_{j=1}^{2} \Delta_j \sigma_j^z - \chi \sigma_1^z \sigma_2^z + J \prod_{j=1}^{2} [\sigma_j^+ e^{2\beta_j (a^\dagger - a)} + \text{H.c.}], \tag{10}$$

where $\chi = 4 g_1 g_2/\omega$ is the $\sigma_1^z \sigma_2^z$ coupling strength between two qubits. Given that $\beta_j \ll 1$ ($\beta_1 = \beta_2 = 0.025$), the last term in Eq. (10) can be expanded to first order in β_j. Therefore, H_{s1} can be approximately written as

$$H_{s2} \simeq \omega a^\dagger a + \frac{1}{2}\sum_{j=1}^{2} \Delta_j \sigma_j^z - \chi \sigma_1^z \sigma_2^z + J[(\sigma_1^+ + \sigma_1^-) + 2\beta_1 (\sigma_1^+ - \sigma_1^-)(a^\dagger - a)] \times [(\sigma_2^+ + \sigma_2^-) + 2\beta_2 (\sigma_2^+ - \sigma_2^-)(a^\dagger - a)]. \tag{11}$$

The last term describes various types of multiexcitation interactions among the qubits and the field, such as $\sigma_1^+ \sigma_2^+ a$ and $\sigma_1^+ \sigma_2^+ a^2$. To observe the effects of the counter-rotating terms in the dipole-dipole coupling, here we assume that the dipole-dipole coupling $J \ll \min\{\Delta_j, \Delta_j \pm \omega\}$ ($j = 1,2$) and $\omega = \Delta_1 + \Delta_2$. Employing the commutation relations $[\sigma_1^z \sigma_2^z, \sigma_1^\pm \sigma_2^\pm] = 0$ and applying the unitary transformation

$$U = \exp\left[-i\left(\omega a^\dagger a + \frac{1}{2}\sum_{j=1}^{2} \Delta_j \sigma_j^z - \chi \sigma_1^z \sigma_2^z\right) t\right] \tag{12}$$

to the Hamiltonian in Eq. (11) for the time t, we obtain the resonant Hamiltonian by neglecting the rapidly oscillating terms

$$H_{\rm eff} = G_s (a \sigma_1^+ \sigma_2^+ + a^\dagger \sigma_1^- \sigma_2^-), \tag{13}$$

with the effective coupling strength

$$G_s = 2J(\beta_1 + \beta_2) = \frac{2J(g_1 + g_2)}{\omega}. \tag{14}$$

We can clearly find that Eq. (13) describes the energy of a photon in a resonator splitting into two parts and simultaneously exciting two qubits. In the original Hamiltonian in Eq. (6), the longitudinal coupling between the jth qubit and the resonator, i.e., $\sigma_j^z a^\dagger$ ($\sigma_j^z a$), corresponds to the creation (annihilation) of a virtual photon in the resonator at a rapid rate ω. The counter-rotating term in the qubit coupling, i.e., $\sigma_1^+ \sigma_2^+$ ($\sigma_1^- \sigma_2^-$), describes the process of simultaneously exciting (deexciting) two qubits. This term does not conserve the excitation number and is also a virtual process oscillating at a high frequency ($\Delta_1 + \Delta_2$). However, as shown in Fig. 3, these excitation-number-nonconserving processes can be combined together to form four resonant transition processes. The coherent-transfer rate between the states $|n+1,g,g\rangle$ and $|n,e,e\rangle$ is $\sqrt{n+1}G_s$, with $|n,g,g\rangle$ and $|n+1,e,e\rangle$ being two intermediate states, respectively. In contrast to conventional QED problems, where we neglect the counter-rotating terms, here $H_{\rm CR}$ plays a key role in exciting the two qubits simultaneously, while the resonant terms $H_{\rm R}$ have no effect. Therefore, the RWA is not valid here, even if the couplings are not in the ultrastrong-coupling regime.

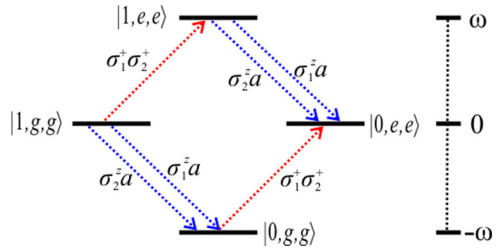

FIG. 3. Sketch of the high-order transitions between the states $|1,g,g\rangle$ and $|0,e,e\rangle$. The four transition paths, allowed by the longitudinal couplings (blue arrows) $\sigma_j^z a$ and the counter-rotating terms $\sigma_1^+\sigma_2^+$ (red arrows), are mediated by the two states $|0,g,g\rangle$ and $|1,e,e\rangle$. It is seen that the only difference between the two paths (with the same intermediate state) corresponds to different longitudinal couplings, which results in annihilating a virtual photon via the first (at the rate $\beta_1 J$) or second (at the rate $\beta_2 J$) qubits.

By assuming the same parameters as in Fig. 2 and $\Delta_1 = 4$ GHz, the effective coupling strength can be as strong as $G_s = 10$ MHz. Compared with the results in Refs. [33,36], there is only a *single* (rather than *two*) intermediate virtual state $|0,g,g\rangle$ during the process where a single photon excites two atoms. Consequently, the corresponding coupling rates are faster by about one order of magnitude.

C. Adiabatic Landau-Zener transition

In the vicinity of the anticrossing point, we first examine the adiabatic Landau-Zener transition effect [74–76] without considering the dissipative channels. Assume that the atomic transition frequency Δ_1 is linearly dependent in time, i.e.,

$$\Delta_1(t) = \Delta_1(0) + vt, \tag{15}$$

where $\Delta_1(t)$ sweeps through the anticrossing point at a velocity v. In an experiment, it is convenient to tune $\Delta_1(t)$ linearly by changing the flux $\Phi_{x,1}$ through the SQUID loop. We assume that the system is initially in its fourth eigenstate $|\psi_4\rangle \simeq |1,g,g\rangle$. When changing $\Delta_1(t)$ linearly, the system might jump to the lower eigenstate $|\psi_3\rangle$ due to the *diabatic* transition. In other words, this means that the system evolves far away from a quasisteady state and transitions between different eigenstates can occur. The final transition probability to the state $|\psi_3\rangle \simeq |1,g,g\rangle$ ($\Delta > 4$ GHz) can be approximately expressed by the Landau-Zener formula [24,74,75], i.e.,

$$P_{\psi_3} = \exp\left[-2\pi \frac{G_s^2}{dE_\Delta/dt}\right], \tag{16}$$

where $E_\Delta = E_4(t) - E_3(t)$ is the eigenenergy difference between the fourth and third eigenstates, and dE_Δ/dt is the sweeping rate. Here we simply have $dE_\Delta/dt \simeq v$. If the energy-sweeping speed v is extremely slow and satisfies the relation $2\pi G_s^2 \gg v$, the anticrossing point traverses *adiabatically* [24,75]. In this case, the system approximately evolves along the fourth-energy curve, and the system rarely jumps to the third eigenstate after the sweeping, i.e., $P_{\psi_3} \ll 1$.

In Fig. 4, by setting $\Delta_0(t) = 3.84$ GHz and $v = 6 \times 10^{-5}$ (GHz)^2, we numerically simulate the evolution dominated by the Schrödinger equation and plot the probabilities of the states $|1,g,g\rangle$ and $|0,e,e\rangle$ changing with time, respectively.

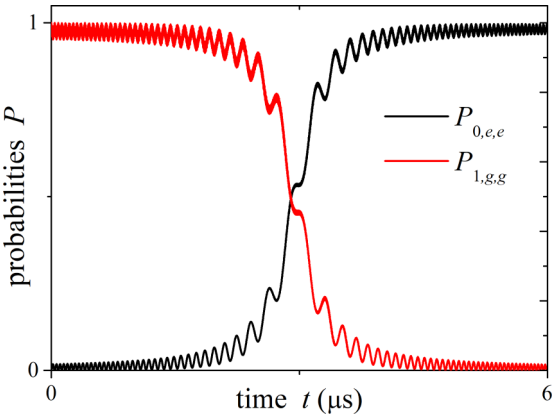

FIG. 4. The time-dependent Landau-Zener transition process is achieved by slowly changing the first-qubit frequency Δ_1 with a sweeping rate $v = 6 \times 10^{-5}$ (GHz)^2. The initial state is $|1,g,g\rangle$ (red curve). Due to the resonant coupling effects, the probability of the initial state is gradually decreased, and the system is adiabatically transferred into the state $|0,e,e\rangle$ (black curve) with the final probability $P_{1,e,e} \simeq 0.99$. The other parameters used here are the same as those in Fig. 2(a).

It can be clearly seen that the probability $P_{0,e,e}$ gradually increases from 0 to ~0.99. The transition time is of the order of several microseconds. For the final states, there is still a low probability $P_{1,g,g}$ because of the extremely weak diabatic-transition effect [75]. During this process, the excitation energy of a single photon is split into two parts to effectively excite the two flux qubits. The dynamics of this Landau-Zener transition provides strong evidence of the resonant coupling between the states $|1,g,g\rangle$ and $|0,e,e\rangle$.

IV. QUANTUM RABI OSCILLATIONS AND INTERFERENCE EFFECTS BETWEEN FOUR TRANSITION PATHS

To examine the deterministic transition between the states $|1,g,g\rangle$ and $|0,e,e\rangle$, the rate of the adiabatic Landau-Zener transition process is extremely slow. Therefore, we can simply observe the Rabi oscillation between these two states.

We assume that the resonator and two qubits are coupled to the vacuum environment and the initial states of the system are their ground states $|0,g,g\rangle$. The coherent electromagnetic field is applied via a one-dimensional (1D) transmission line, which couples to one side of the resonator via a capacitance [77].

We can inject a single photon into the resonator by applying a Gaussian pulse, i.e., to prepare the initial state as $|1,g,g\rangle$, and the corresponding drive has the form

$$H_{\rm drv}(t) = A\frac{\exp\left[-(t-t_0)^2/(2\tau^2)\right]}{\sqrt{2\pi}\,\tau}(ae^{i\omega t} + a^\dagger e^{-i\omega t}), \tag{17}$$

where A, t_0, and τ are the amplitude, central-peak position, and width of a Gaussian pulse. However, for a resonator without nonlinearity, the higher-energy states (for example, $|2,g,g\rangle$) can also be effectively populated. We can employ an ancillary superconducting qubit to induce some nonlinearities of the resonator with a Kerr-type Hamiltonian $H_{\rm Kerr} = \chi_3 a^{\dagger 2} a^2$

[33,78]. Here, χ_3 is the effective Kerr-interaction strength proportional to third-order susceptibility. As a result, the Hamiltonian for the whole system can be written as

$$H_t = H_T + H_{\rm Kerr} + H_{\rm drv}(t). \tag{18}$$

A. Modified input-output relation

In standard QED systems, the output and correlation signal are obtained via photodetection methods. As discussed in Refs. [22,25,26,79], when the coupling is in the strong- or ultrastrong-coupling regimes, the eigenstates of the system are the highly dressed states which are different from the bare eigenstates of the resonator and qubits, and the standard input-output relation fails to describe the output field. For example, the output-field photon flux is no longer proportional to the conventional first-order correlation functions of the cavity operators [25]. By contrast to this, the output field from the cavity is linked to the electric-field operator $X = a + a^\dagger$ (rather than the annihilation operator a) [25,80,81].

To discuss problems more explicitly and consider more general cases, we employ the modified formula of the input-output relation and correlation functions in the following discussions. Defining the positive- and negative-frequency [79] components of the operator X as

$$X^+ = \sum_{j,k>j} X_{jk}|\psi_j\rangle\langle\psi_k|, \quad X^- = (X^+)^\dagger, \tag{19}$$

where $X_{jk} = \langle\psi_j|(a + a^\dagger)|\psi_k\rangle$, the modified input-output relation under the Markov approximation can be reexpressed as

$$A_{\rm out} = A_{\rm in} - \sqrt{\kappa}X^+, \tag{20}$$

where $A_{\rm in}$ is the input vacuum noise [25,80,81], κ is the photon escape rate from the resonator [77], and $A_{\rm out}$ is the output field operator of the form [79]

$$A_{\rm out}(t) = \frac{1}{2\sqrt{\pi\omega\upsilon}}\int_0^\infty d\omega' a'(\omega',t_1)e^{-i\omega'(t-t_1)} + \text{H.c.}, \tag{21}$$

where υ is the phase velocity of the mode ω, and a' is the annihilation operator of the continuous mode with frequency ω' outside the resonator. The output photon flux can be expressed as $\Theta = \kappa\langle X^- X^+\rangle$.

B. Rabi oscillations based on numerically simulating the master equation

Under the Born-Markov approximation and assuming that the resonator and the qubits are coupled to the zero-temperature vacuum reservoir, the evolution for the system can be described by the master equation of the Lindblad form [24,26],

$$\frac{d\rho(t)}{dt} = -i[H_t,\rho(t)] + \kappa D[X^+]\rho(t) + \sum_{j=1,2}\Gamma_j D[C_j^+]\rho(t), \tag{22}$$

where $D[O]\rho(t) = [2O\rho(t)O^\dagger - O^\dagger O\rho(t) - \rho(t)O^\dagger O]/2$ is the Lindblad superoperator, and Γ_j is the decay rate of the jth qubit. Our proposal requires *only longitudinal* couplings between the qubits and resonator, rather than *both* longitudinal and transverse couplings used in Ref. [33]. Thus, the flux qubits could now work at their optimal points, and the pure-dephasing rates induced by flux noise can be minimized, as discussed in Refs. [37,38,63]. The coherence time of a flux qubit can be of several μs. Here we assume that $\Gamma_1 = \Gamma_2 = 0.2$ MHz. In an experiment, a superconducting resonator with quality factor over 10^4 can be easily fabricated [82]. We consider the decay rate of the resonator to be $\kappa = 0.4$ MHz ($Q = 2\times10^4$). Therefore, under current experimental approaches, the coherent-transition rate G_s can easily overwhelm all the decoherence channels in our proposal.

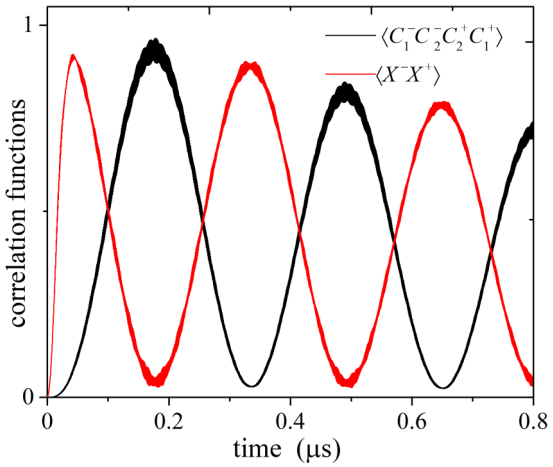

FIG. 5. The intraresonator photon number $\langle X^- X^+\rangle$ (red curve) and zero-delay two-qubit correlation function $G_q^{(2)}(0)$ (black curve) vs time based on numerically solving the master equation (22) with the decay rates $\Gamma_1 = \Gamma_2 = 0.2$ MHz and $\kappa = 0.4$ MHz. The Kerr nonlinearity is assumed to be $\chi_3 = 120$ MHz. The initial state is $|0,g,g\rangle$. The Gaussian pulse parameters are $t_0 = 0$, $\tau = 0.02$ μs, and $A/(\sqrt{2\pi}\tau) = 50$ MHz. Other parameters are the same as those in Fig. 2(a) with $\Delta_1 = 4$ GHz.

The emission field for the jth qubit is proportional to the zero-time delay correlation function $\langle C^- C^+\rangle$ [22], where

$$C_j^+ = \sum_{i,k>i} C_{j,ik}|\psi_i\rangle\langle\psi_k|, \quad C_j^- = (C_j^+)^\dagger, \tag{23}$$

with the coefficients $C_{j,ik} = \langle\psi_i|(\sigma_+^j + \sigma_-^j)|\psi_k\rangle$. It can be clearly found that the emission operator is also divided into positive- and negative-frequency parts. The zero-delay two-qubit correlation function

$$G_q^{(2)}(0) = \langle C_1^- C_2^- C_2^+ C_1^+\rangle$$

is proportional to the probability that two qubits are both in their exited states [33].

In Fig. 5, we numerically calculate the photon number $\langle X^- X^+\rangle$ inside the resonator and the two-qubit correlation function $G_q^{(2)}(0)$ changing with time. It can be seen that due to the Kerr-type nonlinearity, a Gaussian pulse can create a single photon in the resonator and the photon flux can increase rapidly. When $t \gg \tau$, the pump effect of the Gaussian pulse almost vanishes and excitation energies can be coherently transferred between the resonator and two qubits via the Rabi-oscillation process. Around $t \simeq 0.18$ μs, the two-qubit correlation function $G_q^{(2)}(0)$ reaches its highest value $\sim$0.96,

indicating that the two qubits are strongly correlated and both approximately in their exited states. Meanwhile, the photon number $\langle X^- X^+ \rangle$ reaches it lowest value and the injected single photon is effectively converted into the excitations of two qubits. The reversible evolution between $G_q^{(2)}(0)$ and $\langle X^- X^+ \rangle$ is due to the vacuum Rabi oscillations between the states $|1,g,g\rangle$ and $|0,e,e\rangle$. Of course, the amplitude of the oscillations gradually decreases due to the energy-decay channels.

C. Quantum interference between four transition paths

Finally, we discuss another interesting phenomenon. As shown in Fig. 3, we can find that for the two paths with the same intermediate state, the only difference between these paths corresponds to different longitudinal couplings, which lead to creating a virtual photon either via the first qubit ($\sigma_1^z a^\dagger$) or the second qubit ($\sigma_2^z a^\dagger$). The rates of the two paths are $G_1 = J\beta_1$ and $G_2 = J\beta_2$, respectively. The coherent transitions between the initial and final states can be viewed as the interference effect between these paths, i.e., $G_s = 2(G_1 + G_2)$. As discussed in Sec. II, the sign and amplitude of g_j can be easily tuned by changing the flux bias direction and the working position of the energy gap. If g_2 has opposite sign (i,e., with a π-phase difference) but the same amplitude as g_1, the paths become destructive and the coherent transition between the states $|1,g,g\rangle$ and $|0,e,e\rangle$ vanishes. In Fig. 6(a), we plot the anticrossing gap $E_\Delta = E_4 - E_3$ between the third and fourth eigenenergies changing with the relative strength g_2/g_1. It can be clearly seen that E_Δ has a dip (almost zero) at $g_2/g_1 = -1$, indicating that the anticrossing point almost disappears. Note that E_Δ cannot be exactly equal to zero due to higher-order processes. At this point, the states $|1,g,g\rangle$ and $|0,e,e\rangle$ decouple from each other. When $g_2/g_1 > 0$, the anticrossing gap E_Δ increases with g_2 and the transition paths become constructive.

To observe more clearly the quantum destructive effects between these paths, we plot the time-dependent evolution of the photon number $\langle X^- X^+ \rangle$ and the two-qubit correlation function $G_q^{(2)}(0)$. Here we employ the parameters at the dip in Fig. 6(a), i.e., $g_1 = -g_2 = 0.20$ GHz. As shown in Fig. 6(b), the energy can no longer be transferred between the resonator and two qubits, which is different from the Rabi oscillation in Fig. 5. Consequently, a single photon, which is excited by a Gaussian pulse, decays to the vacuum environment (red curve) and the two-qubit correlation function $G_q^{(2)}(0)$ is always zero (black curves). In such conditions, the coherent transfer between the states $|1,g,g\rangle$ and $|0,e,e\rangle$ vanishes due to the destructive effect, and the counter-rotating-term effect (that a single photon excites two qubits simultaneously) cannot be observed. Therefore, in an experiment, we can simply change the *relative sign and amplitude* of the flux sensitivity R_j to observe either destructive or constructive interference effects caused by the counter-rotating terms.

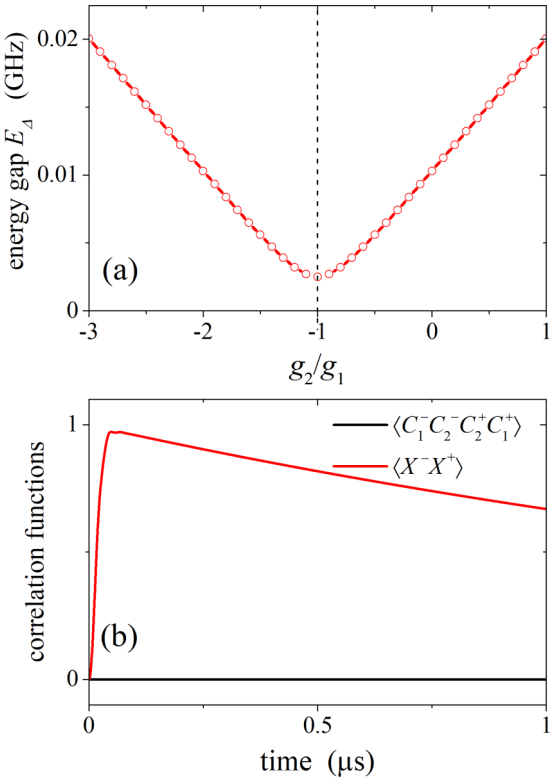

FIG. 6. (a) The energy gap (difference) between the third and fourth eigenenergies, $E_\Delta = E_4 - E_3$, vs the relative coupling strength g_2/g_1 ($g_1 = 0.20$ GHz). At $g_2/g_1 = -1$ (vertical dashed line), the gap almost vanishes. (b) Time evolutions of the photon number $\langle X^- X^+ \rangle$ (red curve) and two-qubit correlation function $G_q^{(2)}(0)$ (black curve), which always vanishes. Here we set $g_1 = -g_2 = 0.20$ GHz. The Rabi oscillation disappears here due to the destructive interference effect between the transition paths. Other parameters are the same as those in Fig. 5.

V. DISCUSSION AND CONCLUSIONS

In this paper, we have investigated pure effects of the counter-rotating terms in the dipole-dipole coupling between two superconducting qubits. The theoretical analysis shows that when these two qubits are longitudinally coupled with the same resonator, the energy of a single photon can effectively excite two qubits simultaneously. By discussing the anticrossing points around the resonant regime, we find that this coherent transition process results from the counter-rotating terms and has no relation to the resonant coupling terms between two qubits. In fact, our results throughout this paper show that when dealing with a QED system containing longitudinal couplings, we should examine the energy spectrum of the system carefully before adopting the standard RWA. The counter-rotating terms might play an important role in the physical dynamics of the whole system.

Moreover, we have demonstrated the Landau-Zener transition effects and Rabi oscillations between the states $|1,g,g\rangle$ and $|0,e,e\rangle$, which are clear signatures of the resonant coupling between these two states. The energy of a single photon can be divided to simultaneously excite two qubits via the *longitudinal* couplings and the counter-rotating terms. Moreover, this process is combined with four transition paths, and there can be quantum interference between these paths. We discussed how to control the system to achieve either destructive or constructive interference effects. By discussing the experimentally feasible parameters, we find it is possible to implement our proposal and observe these quantum effects based on current state-of-the-art circuit-QED systems.

In fact, if we consider a more general case with $n\omega = \Delta_1 + \Delta_2$ when deriving the resonant terms in Eq. (11), we can expand this formula to its nth order. In such conditions, a more general resonant Hamiltonian

$$H_{\rm eff}^{(n)} = G_s^{(n)}[a^n\sigma_1^+\sigma_2^+ + (a^\dagger)^n\sigma_1^-\sigma_2^-], \tag{24}$$

which describes higher-order effects when n photons excite two qubits simultaneously, might produce observable quantum effects. However, we should note that the effective rate $G_s^{(n)}$ decreases quickly with increasing n, which might be overwhelmed by the nonresonant-oscillating terms and decoherence processes.

We should emphasize that our proposal here can be a convenient platform to observe pure quantum effects of the counter-rotating terms. As we discussed above, these high-order transitions only contain a single intermediate state, and the rate is much faster compared with the proposals in Refs. [33,36]. Therefore, the tripartite interaction in Eq. (13) provides a different way to prepare a type of Greenberger-Horne-Zeilinger (GHZ) state [83], $(|1,g,g\rangle + |0,e,e\rangle)/\sqrt{2}$ (see Fig. 5). Moreover, if we can prepare two qubits in their excited states, a single-photon output jointly emitted by two qubits can also be obtained via this method. Therefore, this proposal might also be exploited for quantum information processing (including error-correction codes [35]) and quantum optics in the microwave regime.

ACKNOWLEDGMENTS

We thank A. F. Kockum and S. Savasta for discussions and useful comments. X.W. and H.R.L. were supported by the Natural Science Foundation of China under Grant No. 11774284. A.M. and F.N. acknowledge the support of a grant from the John Templeton Foundation. F.N. was partially supported by the MURI Center for Dynamic Magneto-Optics via the AFOSR Award No. FA9550-14-1-0040, the Japan Society for the Promotion of Science (KAKENHI), the IMPACT program of JST, JSPS-RFBR Grant No. 17-52-50023, CREST Grant No. JPMJCR1676, and RIKEN-AIST Challenge Research Fund.

[1] F. Bloch and A. Siegert, Magnetic resonance for nonrotating fields, Phys. Rev. **57**, 522 (1940).
[2] E. T. Jaynes and F. W. Cummings, Comparison of quantum and semiclassical radiation theories with application to the beam maser, Proc. IEEE **51**, 89 (1963).
[3] B. W. Shore and P. L. Knight, The Jaynes-Cummings model, J. Mod. Opt. **40**, 1195 (1993).
[4] E. K. Irish, Generalized Rotating-Wave Approximation for Arbitrarily Large Coupling, Phys. Rev. Lett. **99**, 173601 (2007).
[5] M. O. Scully and M. S. Zubairy, *Quantum Optics* (Cambridge University Press, Cambridge, 1997).
[6] A. A. Anappara, S. De Liberato, A. Tredicucci, C. Ciuti, G. Biasiol, L. Sorba, and F. Beltram, Signatures of the ultrastrong light-matter coupling regime, Phys. Rev. B **79**, 201303(R) (2009).
[7] P. Forn-Díaz, J. Lisenfeld, D. Marcos, J. J. García-Ripoll, E. Solano, C. J. P. M. Harmans, and J. E. Mooij, Observation of the Bloch-Siegert Shift in a Qubit-Oscillator System in the Ultrastrong Coupling Regime, Phys. Rev. Lett. **105**, 237001 (2010).
[8] T. Niemczyk *et al.*, Circuit quantum electrodynamics in the ultrastrong-coupling regime, Nat. Phys. **6**, 772 (2010).
[9] M. Geiser, F. Castellano, G. Scalari, M. Beck, L. Nevou, and J. Faist, Ultrastrong Coupling Regime and Plasmon Polaritons in Parabolic Semiconductor Quantum Wells, Phys. Rev. Lett. **108**, 106402 (2012).
[10] G. Scalari *et al.*, Ultrastrong coupling of the cyclotron transition of a 2D electron gas to a THz metamaterial, Science **335**, 1323 (2012).
[11] A. Baust *et al.*, Ultrastrong coupling in two-resonator circuit QED, Phys. Rev. B **93**, 214501 (2016).
[12] P. Forn-Díaz, J. J. García-Ripoll, B. Peropadre, J.-L. Orgiazzi, M. A. Yurtalan, R. Belyansky, C. M. Wilson, and A. Lupaşcu, Ultrastrong coupling of a single artificial atom to an electromagnetic continuum in the nonperturbative regime, Nat. Phys. **13**, 39 (2017).
[13] F. Yoshihara, T. Fuse, S. Ashhab, K. Kakuyanagi, S. Saito, and K. Semba, Superconducting qubit-oscillator circuit beyond the ultrastrong-coupling regime, Nat. Phys. **13**, 44 (2017).
[14] Z. Chen *et al.*, Single-photon-driven high-order sideband transitions in an ultrastrongly coupled circuit-quantum-electrodynamics system, Phys. Rev. A **96**, 012325 (2017).
[15] D. Braak, Integrability of the Rabi Model, Phys. Rev. Lett. **107**, 100401 (2011).
[16] X. Gu, A. F. Kockum, A. Miranowicz, Y.-x. Liu, and F. Nori, Microwave photonics with superconducting quantum circuits, Phys. Rep. **718-719**, 1 (2017).
[17] S. Ashhab and F. Nori, Qubit-oscillator systems in the ultrastrong-coupling regime and their potential for preparing nonclassical states, Phys. Rev. A **81**, 042311 (2010).
[18] X. Cao, J. Q. You, H. Zheng, A. G. Kofman, and F. Nori, Dynamics and quantum Zeno effect for a qubit in either a low- or high-frequency bath beyond the rotating-wave approximation, Phys. Rev. A **82**, 022119 (2010).
[19] X. Cao, J. Q. You, H. Zheng, and F. Nori, A qubit strongly coupled to a resonant cavity: Asymmetry of the spontaneous emission spectrum beyond the rotating wave approximation, New J. Phys. **13**, 073002 (2011).
[20] X. Cao, Q. Ai, C.-P. Sun, and F. Nori, The transition from quantum Zeno to anti-Zeno effects for a qubit in a cavity by varying the cavity frequency, Phys. Lett. A **376**, 349 (2012).
[21] J. Casanova, G. Romero, I. Lizuain, J. J. García-Ripoll, and E. Solano, Deep Strong Coupling Regime of the Jaynes-Cummings Model, Phys. Rev. Lett. **105**, 263603 (2010).
[22] L. Garziano, R. Stassi, V. Macrì, A. F. Kockum, S. Savasta, and F. Nori, Multiphoton quantum Rabi oscillations in ultrastrong cavity QED, Phys. Rev. A **92**, 063830 (2015).
[23] X. Wang, A. Miranowicz, H.-R. Li, and F. Nori, Multiple-output microwave single-photon source using superconducting circuits with longitudinal and transverse couplings, Phys. Rev. A **94**, 053858 (2016).

[24] K. K. W. Ma and C. K. Law, Three-photon resonance and adiabatic passage in the large-detuning Rabi model, Phys. Rev. A **92**, 023842 (2015).
[25] A. Ridolfo, M. Leib, S. Savasta, and M. J. Hartmann, Photon Blockade in the Ultrastrong Coupling Regime, Phys. Rev. Lett. **109**, 193602 (2012).
[26] A. Ridolfo, S. Savasta, and M. J. Hartmann, Nonclassical Radiation from Thermal Cavities in the Ultrastrong Coupling Regime, Phys. Rev. Lett. **110**, 163601 (2013).
[27] M.-J. Hwang, R. Puebla, and M. B. Plenio, Quantum Phase Transition and Universal Dynamics in the Rabi Model, Phys. Rev. Lett. **115**, 180404 (2015).
[28] A. F. Kockum, V. Macrì, L. Garziano, S. Savasta, and F. Nori, Frequency conversion in ultrastrong cavity QED, Sci. Rep. **7**, 5313 (2017).
[29] M.-J. Hwang, M.-S. Kim, and M.-S. Choi, Recurrent Delocalization and Quasiequilibration of Photons in Coupled Systems in Circuit Quantum Electrodynamics, Phys. Rev. Lett. **116**, 153601 (2016).
[30] A. Le Boité, M.-J. Hwang, H. Nha, and M. B. Plenio, Fate of photon blockade in the deep strong-coupling regime, Phys. Rev. A **94**, 033827 (2016).
[31] W. Denk, J. H. Strickler, and W. W. Webb, Two-photon laser scanning fluorescence microscopy, Science **248**, 73 (1990).
[32] P. T. C. So, C. Y. Dong, B. R. Masters, and K. M. Berland, Two-photon excitation fluorescence microscopy, Annu. Rev. Biomed. Eng. **2**, 399 (2000).
[33] L. Garziano, V. Macrì, R. Stassi, O. Di Stefano, F. Nori, and S. Savasta, One Photon Can Simultaneously Excite two or More Atoms, Phys. Rev. Lett. **117**, 043601 (2016).
[34] A. F. Kockum, A. Miranowicz, V. Macrì, S. Savasta, and F. Nori, Deterministic quantum nonlinear optics with single atoms and virtual photons, Phys. Rev. A **95**, 063849 (2017).
[35] R. Stassi, V. Macrì, A. F. Kockum, O. Di Stefano, A. Miranowicz, S. Savasta, and F. Nori, Quantum nonlinear optics without photons, Phys. Rev. A **96**, 023818 (2017).
[36] P. Zhao, X.-S. Tan, H.-F. Yu, S.-L. Zhu, and Y. Yu, Simultaneously exciting two atoms with photon-mediated Raman interactions, Phys. Rev. A **95**, 063848 (2017).
[37] A. Fedorov, A. K. Feofanov, P. Macha, P. Forn-Díaz, C. J. P. M. Harmans, and J. E. Mooij, Strong Coupling of a Quantum Oscillator to a Flux Qubit at its Symmetry Point, Phys. Rev. Lett. **105**, 060503 (2010).
[38] M. Stern, G. Catelani, Y. Kubo, C. Grezes, A. Bienfait, D. Vion, D. Esteve, and P. Bertet, Flux Qubits with Long Coherence Times for Hybrid Quantum Circuits, Phys. Rev. Lett. **113**, 123601 (2014).
[39] Y. Makhlin, G. Schön, and A. Shnirman, Quantum-state engineering with Josephson-junction devices, Rev. Mod. Phys. **73**, 357 (2001).
[40] J. Q. You and F. Nori, Superconducting circuits and quantum information, Phys. Today **58**(11), 42 (2005).
[41] Y.-x. Liu, J. Q. You, L. F. Wei, C. P. Sun, and F. Nori, Optical Selection Rules and Phase-Dependent Adiabatic State Control in a Superconducting Quantum Circuit, Phys. Rev. Lett. **95**, 087001 (2005).
[42] J. Clarke and F. K. Wilhelm, Superconducting quantum bits, Nature (London) **453**, 1031 (2008).
[43] L. DiCarlo *et al.*, Preparation and measurement of three-qubit entanglement in a superconducting circuit, Nature (London) **467**, 574 (2010).
[44] J. Q. You and F. Nori, Atomic physics and quantum optics using superconducting circuits, Nature (London) **474**, 589 (2011).
[45] I. Buluta, S. Ashhab, and F. Nori, Natural and artificial atoms for quantum computation, Rep. Prog. Phys. **74**, 104401 (2011).
[46] Z.-L. Xiang, S. Ashhab, J. Q. You, and F. Nori, Hybrid quantum circuits: Superconducting circuits interacting with other quantum systems, Rev. Mod. Phys. **85**, 623 (2013).
[47] I. M. Georgescu, S. Ashhab, and F. Nori, Quantum simulation, Rev. Mod. Phys. **86**, 153 (2014).
[48] C. H. van der Wal *et al.*, Quantum superposition of macroscopic persistent-current states, Science **290**, 773 (2000).
[49] Y.-x. Liu, L. F. Wei, and F. Nori, Tomographic measurements on superconducting qubit states, Phys. Rev. B **72**, 014547 (2005).
[50] M. Neeley *et al.*, Process tomography of quantum memory in a Josephson-phase qubit coupled to a two-level state, Nat. Phys. **4**, 523 (2008).
[51] Y.-F. Chen, D. Hover, S. Sendelbach, L. Maurer, S. T. Merkel, E. J. Pritchett, F. K. Wilhelm, and R. McDermott, Microwave Photon Counter Based on Josephson Junctions, Phys. Rev. Lett. **107**, 217401 (2011).
[52] K. Inomata, Z. R. Lin, K. Koshino, W. D. Oliver, J. S. Tsai, T. Yamamoto, and Y. Nakamura, Single microwave-photon detector using an artificial Λ-type three-level system, Nat. Commun. **7**, 12303 (2016).
[53] M. A. Sillanpää, J. Li, K. Cicak, F. Altomare, J. I. Park, R. W. Simmonds, G. S. Paraoanu, and P. J. Hakonen, Autler-Townes Effect in a Superconducting Three-Level System, Phys. Rev. Lett. **103**, 193601 (2009).
[54] X. Wang, H.-r. Li, D.-x. Chen, W.-x. Liu, and F.-l. Li, Tunable electromagnetically induced transparency in a composite superconducting system, Opt. Commun. **366**, 321 (2016).
[55] X. Gu, S.-N. Huai, F. Nori, and Y.-x. Liu, Polariton states in circuit QED for electromagnetically induced transparency, Phys. Rev. A **93**, 063827 (2016).
[56] M. Hofheinz *et al.*, Generation of Fock states in a superconducting quantum circuit, Nature (London) **454**, 310 (2008).
[57] M. Hofheinz *et al.*, Synthesizing arbitrary quantum states in a superconducting resonator, Nature (London) **459**, 546 (2009).
[58] S. P. Premaratne, F. C. Wellstood, and B. S. Palmer, Microwave photon Fock state generation by stimulated Raman adiabatic passage, Nat. Commun. **8**, 14148 (2017).
[59] A. Blais, R.-S. Huang, A. Wallraff, S. M. Girvin, and R. J. Schoelkopf, Cavity quantum electrodynamics for superconducting electrical circuits: An architecture for quantum computation, Phys. Rev. A **69**, 062320 (2004).
[60] J. E. Mooij, T. P. Orlando, L. Levitov, L. Tian, C. H. van der Wal, and S. Lloyd, Josephson persistent-current qubit, Science **285**, 1036 (1999).
[61] T. P. Orlando, J. E. Mooij, L. Tian, C. H. van der Wal, L. S. Levitov, S. Lloyd, and J. J. Mazo, Superconducting persistent-current qubit, Phys. Rev. B **60**, 15398 (1999).
[62] J. Q. You, Y.-x. Liu, C. P. Sun, and F. Nori, Persistent single-photon production by tunable on-chip micromaser with a superconducting quantum circuit, Phys. Rev. B **75**, 104516 (2007).

[63] F. G. Paauw, A. Fedorov, C. J. P. M. Harmans, and J. E. Mooij, Tuning the Gap of a Superconducting Flux Qubit, Phys. Rev. Lett. **102**, 090501 (2009).

[64] A. O. Niskanen, K. Harrabi, F. Yoshihara, Y. Nakamura, and J. S. Tsai, Spectroscopy of three strongly coupled flux qubits, Phys. Rev. B **74**, 220503 (2006).

[65] M. Grajcar *et al.*, Four-Qubit Device with Mixed Couplings, Phys. Rev. Lett. **96**, 047006 (2006).

[66] R. Harris, T. Lanting, A. J. Berkley, J. Johansson, M. W. Johnson, P. Bunyk, E. Ladizinsky, N. Ladizinsky, T. Oh, and S. Han, Compound Josephson-junction coupler for flux qubits with minimal crosstalk, Phys. Rev. B **80**, 052506 (2009).

[67] D. V. Averin and C. Bruder, Variable Electrostatic Transformer: Controllable Coupling of Two Charge Qubits, Phys. Rev. Lett. **91**, 057003 (2003).

[68] M. Wallquist, J. Lantz, V. S. Shumeiko, and G. Wendin, Superconducting qubit network with controllable nearest-neighbour coupling, New J. Phys. **7**, 178 (2005).

[69] R. Harris *et al.*, Sign- and Magnitude-Tunable Coupler for Superconducting Flux Qubits, Phys. Rev. Lett. **98**, 177001 (2007).

[70] D. I. Tsomokos, S. Ashhab, and F. Nori, Using superconducting qubit circuits to engineer exotic lattice systems, Phys. Rev. A **82**, 052311 (2010).

[71] B. Yurke and J. S. Denker, Quantum network theory, Phys. Rev. A **29**, 1419 (1984).

[72] A. A. Clerk, M. H. Devoret, S. M. Girvin, F. Marquardt, and R. J. Schoelkopf, Introduction to quantum noise, measurement, and amplification, Rev. Mod. Phys. **82**, 1155 (2010).

[73] J. B. Majer, F. G. Paauw, A. C. J. ter Haar, C. J. P. M. Harmans, and J. E. Mooij, Spectroscopy on two Coupled Superconducting Flux Qubits, Phys. Rev. Lett. **94**, 090501 (2005).

[74] C. Zener, Non-adiabatic crossing of energy levels, Proc. R. Soc. London **137**, 696 (1932).

[75] J. R. Rubbmark, M. M. Kash, M. G. Littman, and D. Kleppner, Dynamical effects at avoided level crossings: A study of the Landau-Zener effect using Rydberg atoms, Phys. Rev. A **23**, 3107 (1981).

[76] S. N. Shevchenko, S. Ashhab, and F. Nori, Landau-Zener-Stückelberg interferometry, Phys. Rep. **492**, 1 (2010).

[77] D. L. Underwood, W. E. Shanks, J. Koch, and A. A. Houck, Low-disorder microwave cavity lattices for quantum simulation with photons, Phys. Rev. A **86**, 023837 (2012).

[78] A. J. Hoffman, S. J. Srinivasan, S. Schmidt, L. Spietz, J. Aumentado, H. E. Türeci, and A. A. Houck, Dispersive Photon Blockade in a Superconducting Circuit, Phys. Rev. Lett. **107**, 053602 (2011).

[79] L. Garziano, A. Ridolfo, R. Stassi, O. Di Stefano, and S. Savasta, Switching on and off of ultrastrong light-matter interaction: Photon statistics of quantum vacuum radiation, Phys. Rev. A **88**, 063829 (2013).

[80] M. J. Collett and C. W. Gardiner, Squeezing of intracavity and traveling-wave light fields produced in parametric amplification, Phys. Rev. A **30**, 1386 (1984).

[81] C. W. Gardiner and M. J. Collett, Input and output in damped quantum systems: Quantum stochastic differential equations and the master equation, Phys. Rev. A **31**, 3761 (1985).

[82] A. Megrant *et al.*, Planar superconducting resonators with internal quality factors above one million, Appl. Phys. Lett. **100**, 113510 (2012).

[83] D. M. Greenberger, M. A. Horne, A. Shimony, and A. Zeilinger, Bell's theorem without inequalities, Am. J. Phys. **58**, 1131 (1990).